9-26-2016

Histopathological Characterization of the Dystrophic Phenotype and Development of Therapeutic Candidates for a Gene Therapy Pre-Clinical Study in Dysferlin Deficient Mice

Leticia Fridman
University of Massachusetts Medical School

HISTOPATHOLOGICAL CHARACTERIZATION OF THE DYSTROPHIC PHENOTYPE AND DEVELOPMENT OF THERAPEUTIC CANDIDATES FOR A GENE THERAPY PRE-CLINICAL STUDY IN DYSFERLIN DEFICIENT MICE

A Master's Thesis Presented

By

LETICIA FRIDMAN

Submitted to the Faculty of the

University of Massachusetts Graduate School of Biomedical Sciences, Worcester

in partial fulfillment of the requirements for the degree of

MASTER OF SCIENCE

September 24, 2016

TRANSLATIONAL SCIENCES

HISTOPATHOLOGICAL CHARACTERIZATION OF THE DYSTROPHIC PHENOTYPE AND DEVELOPMENT OF THERAPEUTIC CANDIDATES FOR A GENE THERAPY PRE-CLINICAL STUDY IN DYSFERLIN DEFICIENT MICE

A Master's Thesis Presented

By

LETICIA FRIDMAN

The signatures of the Master's Thesis Committee signify completion and approval as to style and content of the Thesis

_____

Marc Freeman, Ph.D., Chair of Committee

_____

Mary Ellen Lane Ph.D., Member of Committee

_____

Kendall Knight Ph.D., Member of Committee

The signature of the Dean of the Graduate School of Biomedical Sciences signifies that the student has met all Master's degree graduation requirements of the school.

_____

Anthony Carruthers, Ph.D.,

Dean of the Graduate School of Biomedical Sciences

Translational Sciences

September 24, 2016

Acknowledgements

I would like to thank Dr. Robert H. Brown, Jr., DPhil, MD for giving me the opportunity to make contributions to this project that has great potential to better the lives of patients with Limb-girdle muscular dystrophy 2B and Miyoshi Myopathy. His continuous commitment to finding cures to improve the lives of patients suffering from devastating neuromuscular diseases is inspiring. I have learned to apply basic science to medicine and to think of my project in the "grand scheme of things" with a focus on patient needs. Over the years, I have also learned important life lessons from working with Bob and seeing him interact with his ALS patients. I move forward with a huge amount of both intellectual and personal growth, for which I am very grateful.

I would like to thank Marc Freeman, Ph.D., for all of his insightful suggestions and intellectual input while being a member and Chair of my TRAC committee. I would also like to give Marc and even larger thank you for being supportive and giving me some of the most constructive advice along the way. It has been a true privilege to work with Marc.

I would like to thank Mary Ellen Lane, Ph.D., Associate Dean of GSBS Curriculum and Academic Affairs for providing me with academic support and advice during all of my phases as a graduate student. Mary Ellen has made a significant positive impact on me and continues to make meaningful contributions and improvements for GSBS students at UMass.

I also would like to thank Ken Knight for his advice and input over the years, for inviting me and allowing me to invite myself to every GSBS Thursday night recruitment dinner at the Beechwood or to any GSBS event with free food, and especially, for laughing with me about it.

Most importantly, I would like to thank my family for their encouragement, support, motivation, and love throughout my life. I would be nowhere without all of you.

ABSTRACT

Dysferlin deficient muscular dystrophy is a devastating disease that leads to loss of mobility and quality of life in patients. Dysferlin is a 230 kD protein primarily expressed in skeletal muscle that functions in membrane resealing. Dysferlin loss of function leads to a decrease in the membrane resealing response after injury in skeletal muscle, which is thought to cause degeneration of the musculature over time.

Dysferlin cDNA is 7.4 kb and exceeds AAV packaging capacity of ~ 5kb. This thesis focuses on the generation of mini dysferlin mutants that can be packaged in AAV for downstream testing of therapeutic efficacy. In addition, this thesis creates the groundwork for preclinical studies in mice that can potentially be translated to human patients. A mouse model for dysferlin deficiency was characterized and key disease phenotypes were identified. In addition, cell lines carrying a genetically encoded calcium indicator protein, gCaMP, were established to measure mini dysferlin resealing capacity and for downstream testing *in vivo*.

TABLE OF CONTENTS

LIST OF FIGURES

LIST OF ABBREVIATIONS

AAV	adeno-associated virus
C. elegans	Caenorhabditis elegans
Ca^{2+}	calcium
cDNA	complimentary deoxyribonucleic acid
C2	protein kinase C calcium-binding domain
DMAT	Distal Myopathy with Anterior Tibialis onset
Dysf	dysferlin
EM	electron microscopy
FER-1	ferlin-1
gCaMP	green fluorescent protein, calmodulin, myosin light chain kinase, peptide
IACUC	Institutional Animal Care and Use Committee
ITR	Inverted Terminal Repeat
kb	kilobase pairs
kD	kilodaltons
LGMD2B	Limb-Girdle Muscular Dystrophy 2B
MG53	Mitsu-gumin 53
MM	Miyoshi Myopathy
rAAV	recombinant adeno-associated virus
ssDNA	single stranded deoxyribonucleic acid
SNARE	SNAP (Soluble NSF Attachment Protein) REceptor
VP	viral protein
WT	wild-type

CHAPTER I: INTRODUCTION TO DYSFERLIN DEFICIENT MUSCULAR DYSTROPHY

Loss of function mutations in the *dysferlin* gene are the genetic defects found in patients with limb-girdle muscular dystrophy type 2B (LGMD2B), Miyoshi myopathy (MM), and distal myopathy with anterior tibial onset (DMAT) which, are autosomal recessive inherited disorders collectively termed "dysferlinopathies". Dysferlin levels ≤ ~20% in skeletal muscle lead to progressive muscular weakness, atrophy, and necrosis (1). Disease onset usually occurs when patients are in their late teens or early twenties, and at least one-third of patients are wheelchair-bound within 10 years of onset (1,2). The main difference between the three dysferlinopathy phenotypes is the muscle or muscle groups where disease onset occurs: pelvic and shoulder muscles in LGMD2B, gastrocnemius muscle in MM, and anterior tibialis muscle in DMAT (1,2). Over time, disease progression in additional muscle groups regardless of onset is inevitable, and can cause respiratory muscle weakness. Additionally, muscle biopsies from patients reveal variability in fiber sizes, increased connective tissue, necrosis, adipose accumulation, and centrally nucleated fibers (1,2).

According to the Universal Mutation Database (www.umd.be/DYSF), there are 416 pathogenic dysferlin mutations identified from 843 patients around the world to date. Most of these mutations are found in exons and as stated in the database, 33% are missense, 18% nonsense, 28% frameshift, 4% in-frame exonic insertions/deletions, and 17% intronic mutations. There is no particular "hot spot" for dysferlin mutations and

no clear phenotype to genotype correlation has been established for each pathogenic mutation. Interestingly, there are cases where the same mutation in consanguineous individuals leads to two different phenotypes (3). A study by Liu & Brown in 1998 identified dysferlin and described an Italian family where 3 out 5 siblings from unaffected parents developed dysferlinopathy. All three siblings (2 females and 1 male) had one allele carrying a 4265A>G mutation in exon 36 (I1298V) and the other allele carrying a 6497C>T mutation in exon 54 (R2042C)(3). The two daughters were affected by LGMD2B and the son was affected by MM. This strongly suggests that modifiers may influence the phenotype, however, none have been identified.

Dysferlin is a large 230 kD protein that is expressed primarily in mammalian skeletal muscle, but is also found in cardiac muscle, brain tissue, and monocytes (3,4,5). To date, 14 human transcript variants of dysferlin have been identified (www.umd.be/DYSF). Variant 8 (NCBI Reference Sequence: NM_003494.2) contains 6,914 base pairs and encodes a 2088 amino acid protein that is the most commonly found variant in skeletal muscle. Dysferlin, or dystrophy-associated fer1-like protein, was named due to shared homology with *C. elegans* FER-1 protein (3). In *C. elegans,* FER-1 has a direct role in vesicle fusion events during spermatogenesis (3,7). Otoferlin, myoferlin, and 3 uncharacterized fer1-like proteins (fer1L4,5,&6) share close homology with dysferlin in mammalian cells (8). Moreover, mutations in otoferlin are the cause of an autosomal recessive form of deafness (9,10).

Tandem C2 domains are a hallmark feature of ferlin family proteins (6,8). They are conserved sequences found in protein kinase C that bind Ca^{2+} and phospholipids (6,8,11). C2 domains have been well characterized in synaptotagmin, a Ca^{2+}-sensor that participates in synaptic neurotransmitter release by triggering Ca^{2+}-dependent exocytosis (11). Synaptotagmin I is a ~50 kD protein that contains two C2 domains C2A and C2B (6,11). The C2A domain has Ca^{2+} -binding loops composed of 5 aspartate residues and one serine residue that bind 3 Ca^{2+} ions (6,11). The structure of synaptotagmin C2 domains is conserved among ferlin proteins (6). Biochemical studies in otoferlin demonstrate that C2 domains are calcium sensors, which bind SNARE proteins to mediate membrane fusion at the synapses of inner ear hair cells for neurotransmitter release (9,10). Dysferlin contains seven C2 domains A-G, which bind Ca^{2+} and phospholipids similarly to synaptotagmin (6), thus a function for dysferlin in calcium sensing and membrane fusion events is evident.

In skeletal muscle fibers, dysferlin localizes to the sarcolemma (the plasma membrane of muscle cells) and is anchored by its C-terminal transmembrane domain, with the seven C2 domains located inside the cytoplasm (4,5,6). In 2003, two groups reported that dysferlin is directly involved in membrane resealing of sarcolemmal lesions (4,5). This observation was made after using two different techniques to wound the sarcolemma of a dysferlin null muscle cell. One group used a micropipette to carefully injure cultured myotubes and measured calcium influx by utilizing calcium indicator dye Indo1-AM (4). The other group employed a laser-mediated injury method in conjunction

with lipophilic FM1-43 dye to measure resealing based on accumulation of the dye at the site of injury (5).

Dysferlin was the first membrane repair protein identified in skeletal muscle. The membrane repair field arose in the last 20 years with the work of Richard Steinhardt and Paul McNeil. Steinhardt demonstrated that the mechanism for membrane resealing in sea urchin eggs and 3T3 fibroblasts is similar to neurotransmitter release (12). Microinjection of botulinum toxins that cleave SNAREs involved in the fusion step of neurotransmitter release inhibited membrane resealing in sea urchin eggs, thus suggesting Ca^{2+}-dependent exocytosis was required (12). The following key observations leading to the now widely accepted "patch-hypothesis" for membrane resealing were: I.) vesicle accumulation at the site of membrane disruption reminiscent of docked vesicles during neurotransmitter release (15) and II.) The formation of an impermeant barrier after microinjection of [10mM] Ca^{2+} -containing seawater into the cytoplasm of a sea urchin egg (13,14). This barrier was confirmed to be a membrane by electron microscopy and staining with lipophilic dye (13,14). It was hypothesized that vesicle-vesicle fusion events led to its formation due to its unusually large size as visualized by EM (13,14). Interestingly, in the absence of Ca^{2+}, significantly smaller vesicles accumulated at the site of injury and appear to be docked and unable to fuse (13,14). The patch hypothesis states that: upon disruption, vesicle-vesicle and vesicle-plasma membrane fusions occur, resulting in accumulation of large vesicles at the injury site (17). Then, the patch is linked to the membrane *via* vesicle-plasma membrane fusion event (17). The identity of these vesicles is still debated; one group claims that lysosomes are exclusively utilized in the membrane repair pathway, due to localization of Lamp-1, a lysosome-specific protein at the lesion site while (16). Others including McNeil and Steinhardt contend that non-lysosomal

vesicles are also utilized for resealing based on the observations in sea urchin eggs (17). It is conceivable that recruited vesicle type may vary due to several factors such as injury size and/or cell type. Lennon and Brown in 2003 were the first to identify Lamp-1 on the sarcolemma of myotubes after injury in the presence of Ca^{2+}(4). In addition, they reported a decrease in Lamp-1 expression at the sarcolemma after injury in cultured myotubes of dysferlin null mice (4). A recent study in coronary arterial endothelial cells shows that dysferlin promotes lysosome fusion to the plasma membrane *via* its C2A domain (19).

The newest membrane repair associated protein identified, MG53, interacts with dysferlin at the C2A domain (20,21,22). In the last few years, several studies have implicated annexins, caveolin-3, calpain-3, and MG53 in the dysferlin-mediated repair pathway; however, a clear mechanism has yet to emerge (20,21,22,23). A compelling new study by Lek et al 2013, demonstrates that rapid localization to the site of injury is exclusive to MG53 and dysferlin (24). In addition, the study shows that dysferlin is cleaved by calpain into a ~72 kD C-terminal fragment in a Ca^{2+} dependent manner after injury (24). This is particularly interesting because a naturally occurring 73 kD mini-dysferlin containing the last two C2 domains near the C-terminus has been associated with a mild form of dysferlinopathy (23). The discovery of a mini-dysferlin by Krahn et al 2010, which retains the membrane resealing function led to the possibility of AAV-mediated gene replacement therapy for Dysferlinopathy, because AAV does not have the packaging capacity for full-length dysferlin cDNA.

Adeno-associated viruses are small single-stranded DNA viruses that belong to the *Parvoviridae* family. The ~4.7kb ssDNA genome is enclosed in an icosahedral capsid that is comprised of three proteins: VP1, VP2, and VP3 in a 1:1:8 ratio (26,27). The capsid and replication genes are flanked by ITRs that form hairpin structures (26,27,28). In addition, genes encoding proteins required for replication and infection, Rep 78,68,52 and 40, are found in the AAV genome (26,27). Infection begins with AAV binding to the cell surface and entering the host cell through association with one or more host surface receptors or co-receptors depending on the AAV serotype (27). The virus is then endocytosed, and undergoes a structural change in response to the acidic endosomal environment. This promotes escape from the endosome and the virus can then enter the nucleus and replicate its DNA (27). Once nuclear entry occurs, the ssDNA of the gene is converted to dsDNA by either, annealing of + or – strands, or through host repair DNA polymerase (25). Wild-type AAVs are unable to replicate without additional "helpers" such as adenoviruses or herpesviruses, and in their absence, wild-type AAV integrates into the host genome and remains latent (26,27). In recombinant AAV vectors (rAAV), the wild-type ORF encompassing the replication and capsid genes is deleted and the rAAV vector genome contains only the transgene of interest flanked by ITRs (27). When rAAV dsDNA is produced in skeletal muscle, it is kept in a circular form where it can concatemerize and persist as an extrachromosomal element (25,29). rAAV does not encompass any wild-type AAV genes and cannot promote its own integration into the host genome. However, there is evidence that rAAV can integrate into the genome in the presence of host DNA double strand breaks in various tissues such as brain, skeletal muscle, heart, and liver (38). rAAV can also integrate by homologous recombination if the designed vector contains homologous sequences to the host genome (38).

AAV has never been associated with human disease, and due to its unique properties that allow for transgene vector engineering and viral transduction in a wide range of tissues, it has become a very promising vector for gene delivery.

Two groups have exploited the biology of AAV in different ways to express full-length dysferlin in skeletal muscle (29,30). One group utilized the concatemerization property of AAV to achieve full-length dysferlin expression *via* 2 independent vectors each carrying half of the protein (29). In this approach, the coding sequence was split between exons 28 and 29; one vector was packaged with the 5' end of dysferlin cDNA that had an intron carrying a splice donor site, and the other vector contained the 3' end with an intron carrying a splice acceptor site (29). Intramuscular injection of the dual vectors in dysferlin null mice achieved: expression in the muscle, restoration of membrane resealing, and histological improvement. Systemic injections also led to some histological improvements, however, according to their western blot analysis, only 1-4% dysferlin expression compared to WT levels was achieved (29). Therefore, these results imply that in humans, relying on the trans-splicing and concatemerization of dual vectors for transgene expression in the various muscle groups of the body following systemic injection may be ineffective.

Another group sought to exploit the mechanism by which AAV5 mediates delivery of ~8kb genes (30). It was initially reported that this serotype had a large packaging capacity, however, studies have shown that this vector cannot package cDNA larger than 5kb (31). The mechanism by which large gene delivery occurs with

rAAV5 is actually due to homologous recombination of partially packaged vectors (30,31). Intramuscular and regional vascular delivery of dysferlin *via* rAAV5 in dysferlin null mice also achieved functional and histological improvements (30). However, this mode of dysferlin delivery is probably not effective at achieving normal dysferlin expression in every muscle group of the body for patients receiving IV injections, since the homologous recombination frequency in mammalian cells is low. Furthermore, the ratio of partially packaged products delivered to every muscle group cannot be controlled, for example, if there is a higher ratio of either 5' or 3' product, this will affect how many particles can recombine to express full-length dysferlin. Because the feasibility of full-length dysferlin expression achieved in humans using AAV seems limited, the focus of my study is mini-dysferlin treatment for gene replacement therapy. We hypothesize that a partial dysferlin gene containing a set of domains critical for dysferlin function in skeletal muscle can reverse the dystrophic phenotype in dysferlin null mice and therefore, we will explore the therapeutic efficacy of various mini-dysferlin therapeutic candidates to overcome skeletal muscle degeneration associated with dysferlin loss of function.

A recent report suggests a lack of correlation exists between rescue of membrane resealing function and histological improvement in dysferlin null mouse skeletal muscle following mini-dysferlin AAV treatment (32). The repair assay used in this study measured FM1-43 fluorescence uptake at the site of injury. The assumption that dye uptake directly correlates directly with membrane resealing may not be valid. It is possible that FM1-43 dye uptake at the site of injury does not directly measure resealing and therefore is not predictive of therapeutic outcome. One goal of this study is to develop tools for a downstream bioassay that directly measures membrane resealing to

assess mini-dysferlin AAV treatment in dysferlin null mice. It is now well established that membrane resealing is a calcium dependent process (12-17). We believe that measuring calcium influx in *ex vivo* muscle fibers is a more accurate measurement of the membrane resealing process in skeletal muscle cells.

In summary, the aims of this study are: to characterize the dystrophic phenotype in a new dysferlin null mouse strain, to develop mini dysferlin mutants to correct the dystrophic phenotype by AAV delivery, to develop gCaMP6s-Mini dysferlin cell lines to measure resealing function by calcium influx, and to further explore dysferlin biology by assessing mini dysferlin localization in dysferlin null muscle cells.

CHAPTER II: HISTOPATHOLOGICAL CHARACTERIZATION OF DYSFERLIN NULL BLA/J MOUSE STRAIN

Introduction

Various mouse models for dysferlin deficiency are now available (5,29,33). There are differences in age of onset, disease progression, dysferlin levels, and behavior among the mouse models. The SJL model contains a splice-site mutation in Exon 45 which causes an ~85% reduction in dysferlin levels, as confirmed by western blot and quantitative PCR (33). The A/J dysferlin deficient mouse model arose from continuous colony inbreeding at Jackson Laboratory and contains a retrotransposon insertion at the dysferlin locus (33). A/J mice display docile sedentary behavior and become overweight as they age, whereas, SJL mice are aggressive and must be housed separately from one another. SJL and A/J mice contain additional genetic defects aside from dysferlin deficiency due to decades of colony inbreeding and may not be ideal for therapeutic evaluation. The most recent dysferlin null model was created by backcrossing of the A/J strain with a wild-type C57BL6/J strain, resulting in a new strain termed Bla/J (29). These new Bla/J mice contain the A/J retrotransposon insertion at the dysferlin locus in a BL6(WT) background. Unlike A/J and SJL dysferlin null mice, Bla/J mice are active rather than sedentary and do not display aggressive behavior. The Bla/J strain is ideal for therapeutic evaluation with wild-type C57BL6/J controls. This new model has not been extensively characterized.

Results

Gross Anatomy and Histology of Bla/J Musculature

Bla/J mice live up to ~18-20 months of age until euthanization is required due to weight loss and gait irregularities. At this end stage, most hindlimb and forelimb muscle groups have degenerated, with the quadriceps and triceps being the most affected (Figure 1A & B). Gross anatomical examination of the hindlimb musculature at 18 months of age (Figure 1A) reveals more advanced degeneration in the quadriceps than in the gastrocnemius or tibialis anterior muscles of *dysf* -/- Bla/J mice (n=6) when compared to healthy *dysf* +/- age-matched littermate controls (n=4).

H&E staining of 18 month-old Bla/J muscle cross-sections reveal key hallmark features of muscle disease pathology such as fiber shape irregularity, centrally nucleated fibers, macrophage infiltration, fibrosis, and adipose deposits (Figure 1B). Both triceps (Figure 1B, panel A) and quadriceps (Figure 1B, panel B) sections display severe immune cell infiltration around the vasculature and substantial amount of adipose accumulation (n=6). The gastrocnemius and tibialis anterior (Figure 1B, panels C & D) muscle groups appear only mildly affected relative to the triceps and quadriceps, but still contain the presence of centrally nucleated fibers.

Figure 1A: Dysf WT vs. Bla/J Mouse Hindlimb Skeletal Musculature at 18 months

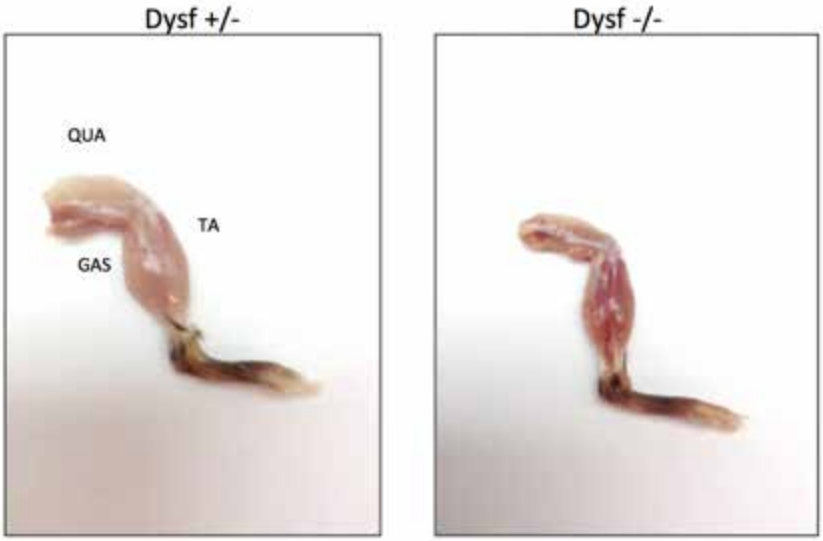

Figure 1B: Dysf -/- Bla/J Mouse Skeletal Muscle Histopathology at 18 months

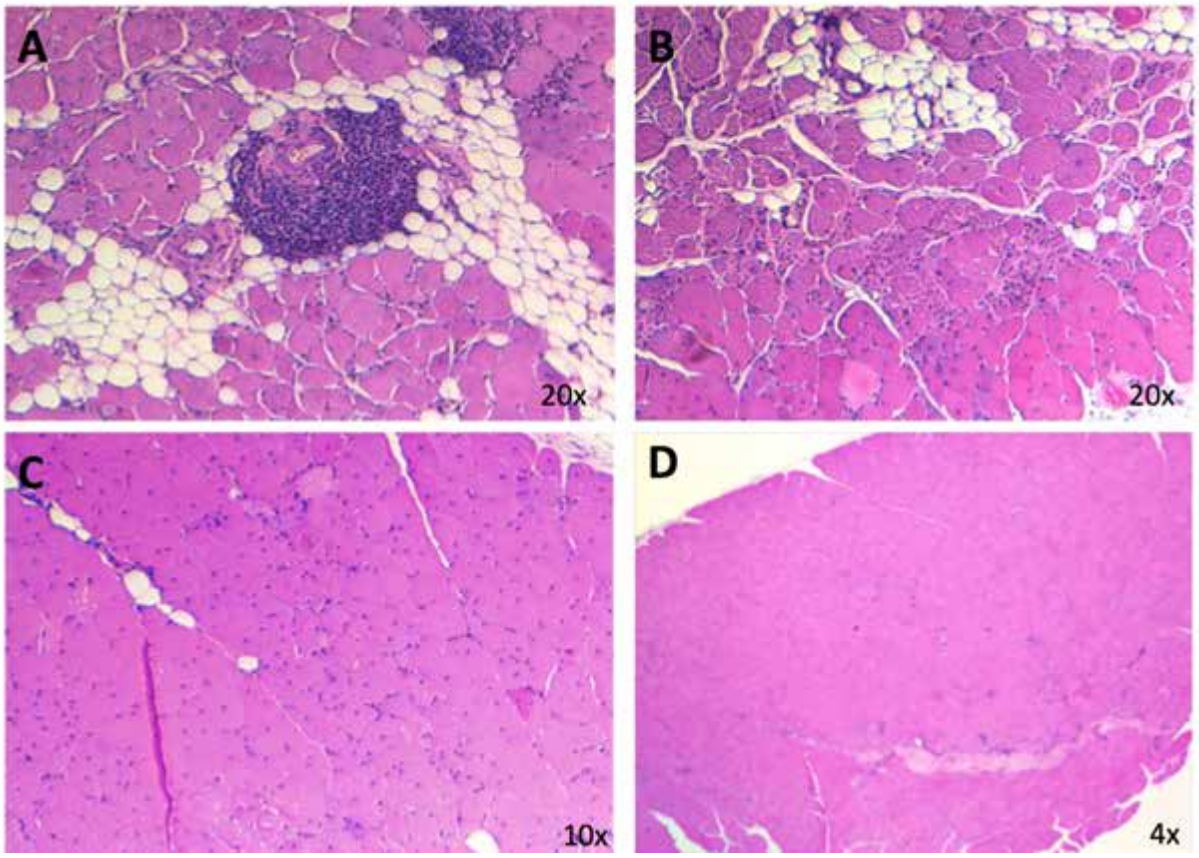

Figure 1A: Gross Anatomy of 18 month-old WT vs. Bla/J hindlimb musculature.
Figure 1B: Bla/J H&E Histology A. Diseased triceps presenting macrophage infiltration (purple mass at image center) and adipose accumulation (white circular patterns) B. quadriceps presenting macrophage infiltration, adipose accumulation, fiber shape irregularity, and centrally nucleated fibers. C. Gastrocnemius section displaying presence of centrally nucleated fibers. D.4x image of Tibialis Anterior shows the entirety of this muscle is only mildly affected.

Membrane Integrity of Bla/J Muscle

Evans blue dye is an azo dye that binds to serum albumin and is not present inside muscle fibers of healthy wild-type mice and dye uptake into skeletal muscle fibers suggests a diseased state of the fiber where sarcolemmal integrity is compromised (43).

Intraperitoneal injections of Evans blue dye were administered to eight-month old dysf -/- Bla/J and wild-type C57BL6/J and tissue was harvested 16 hours post injection (Figure 2 A & B). Upon gross anatomical examination, Evans blue dye is observed to penetrate the skeletal musculature of dysferlin deficient mice, giving them an overall blue appearance (Figure 2A). Because Evans blue emits fluorescence in the red channel, evaluation of dye penetration inside skeletal muscle fibers is viable. Evaluation of dye uptake in various muscle groups in 8 month-old dysf -/- mice reveals that the gastrocnemius and quadriceps have the most dye uptake, which also correlates with more severe histopathology of these two muscle groups as observed by H&E staining at this particular time point (Figure 2B, rows A & B). The next goal was to identify the earliest time point of dye uptake in dysf -/- skeletal muscle. Evans blue dye intraperitoneal injections where administered to 5,6,and 7 month-old dysf -/- Bla/J mice and dye penetration into muscle fibers was evaluated by fluorescence microscopy (Figure 3A). Significant uptake into the gastrocnemius and quadriceps is observed starting at 7 months of age, also correlating with the histopathological deterioration of the muscle as seen on the H&E stains. Deterioration appears more pronounced in the quadriceps than in the gastrocnemius and dye uptake area in the quadriceps appears greater at this time point. Interestingly, when Evans blue dye was administered to end stage 20 month-old dysf -/- Bla/J mice with severe histopathology, only a small amount of dye uptake was observed (Figure 3B).

Figure 2A: Evans Blue Dye Sarcolemmal Permeability in 8 month old Dysf -/- Skeletal Muscle

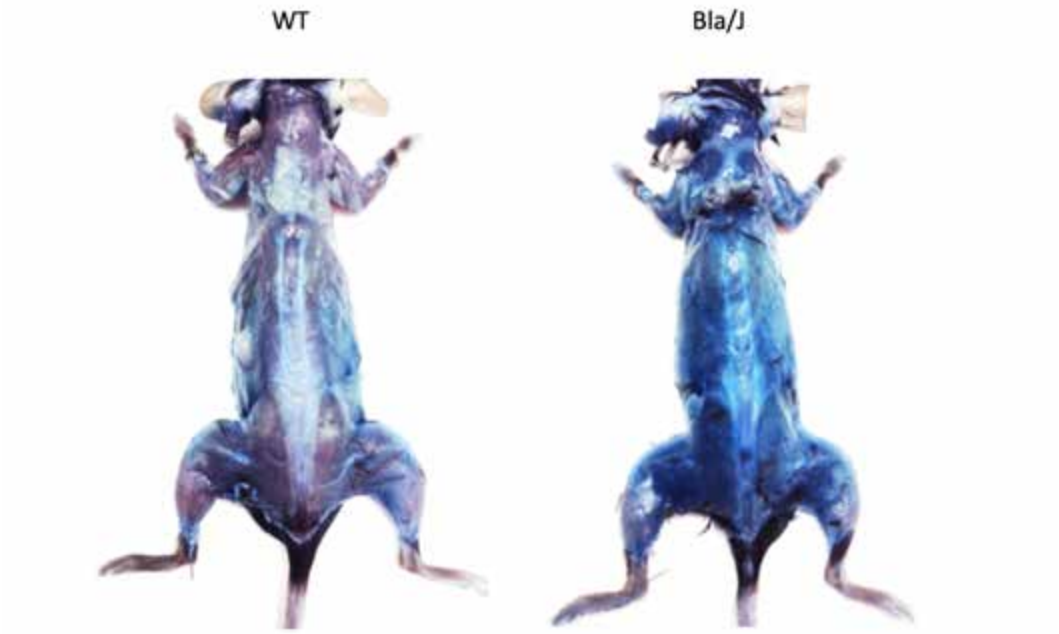

Figure 2B: Evans Blue Dye Uptake in 8 month old Dysf -/- Bla/J Skeletal Muscle

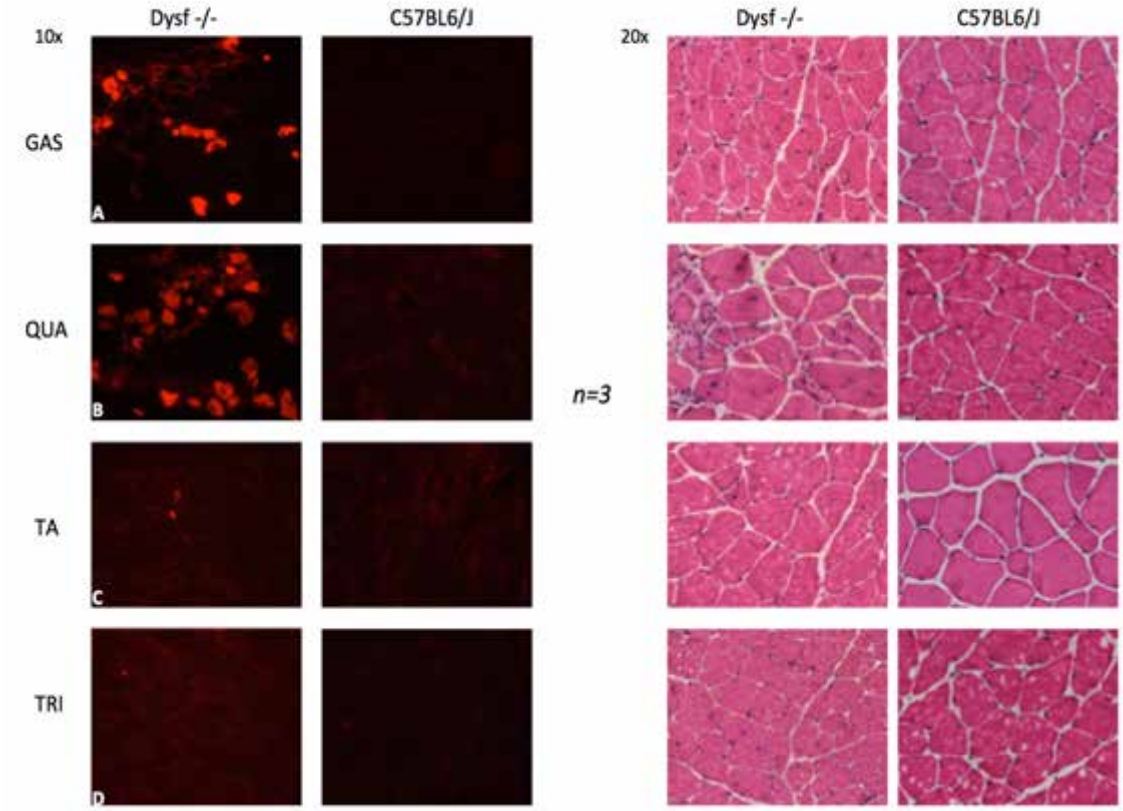

Figure 2A: Gross anatomical evaluation of Evans blue dye uptake into the musculature of dysf -/- and WT mice post injection.
Figure 2B: Histological evaluation of Evans blue dye uptake into muscle fibers of different muscle groups (left panel) and H&E staining (right panel).

Figure 3A: Evans Blue Dye Uptake in Dysf -/- Bla/J Skeletal Muscle

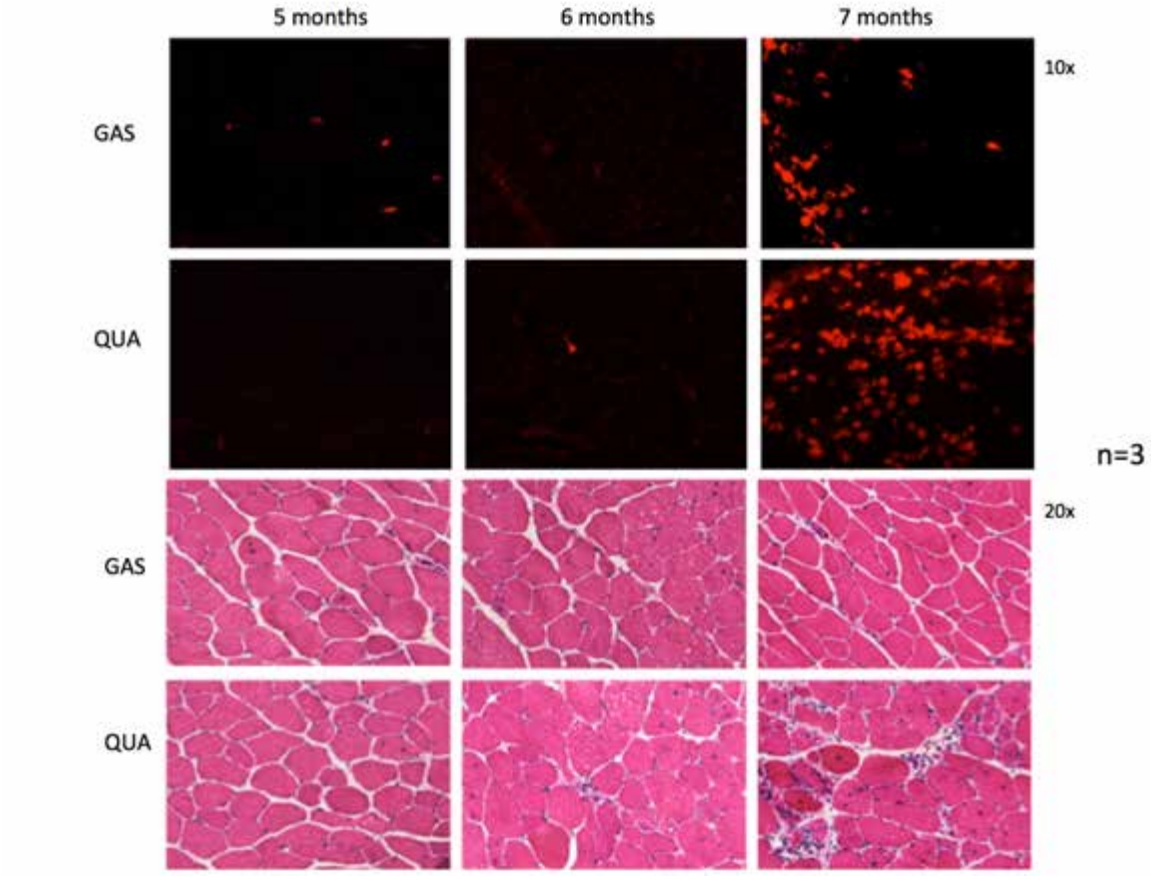

Figure 3B: Evans Blue Dye Uptake in 20 month old Dysf -/- Bla/J mice

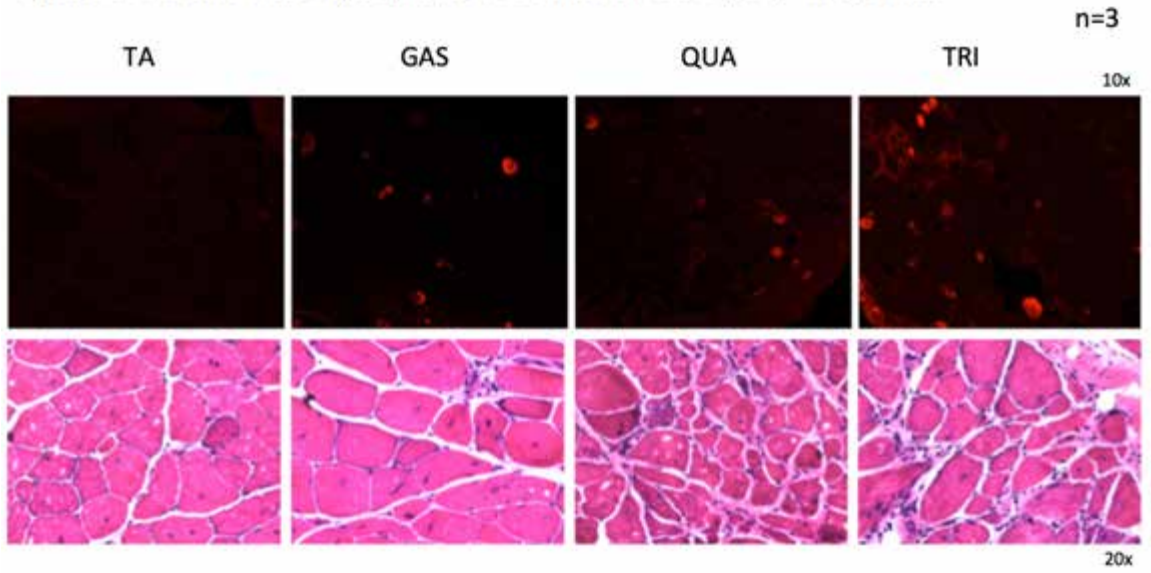

Figure 3A: Evans blue dye uptake into dysf -/- Bla/J gastrocnemius and quadriceps muscles at 5,6,and 7 months of age and H&E stains of disease progression (bottom panel).

Figure 3B: Evans blue dye uptake into tibialis anterior, gastrocnemius, quadriceps, and triceps of 20 month old dysf -/- Bla/J mice and H&E stains of each muscle group (bottom panel.)

Materials and Methods

Mice

All experiments involving mice were approved by the UMass Medical School IACUC. Dysf -/- Bla/J mice and C57BL6/J mice were purchased from Jackson Laboratory and housed in accordance with our IACUC protocol and institutional standards.

Histology

Tissue extracted from mice upon dissection was either fixed in 10% neutral buffered formalin (Sigma cat# HT501128) for 24 hours followed by paraffin embedding and sectioning at 4 um using a Leica microtome (Figure 1B) or fresh-frozen in liquid nitrogen-cooled isopentane (Sigma cat#M32631-4L) and sectioned in OCT medium (Electron Microscopy Sciences cat#62550-12) at 10 um on a Leica cryostat (Figures 2&3). Paraffin embedded sections were deparaffinized with xylene (Sigma cat# 534056-4L) washes and rehydrated in a 100%-70% ethanol gradient for H&E staining. Fresh–frozen sections were washed in 1X PBS (Fisher cat# BP3994) for 5 minutes and stained with hematoxylin (Leica cat#3801562) for 5 minutes, rinsed with tap water, and stained with Eosin (Leica cat#3801602) for two minutes followed by dehydration through a 70%-100% ethanol gradient, followed by two 5 minute xylene washes. Sections were mounted in DPX (Sigma cat# 06522) mounting medium. Images were acquired with a Nikon Ti microscope.

Evans Blue Dye Injections

Evans blue powder (Sigma cat# E2129) was dissolved in 1X PBS at [0.01 mg/uL] and filter sterilized through a 0.22 um Millipore filter. Mice were injected with 100 uL of Evans blue dye in 1X PBS solution per 10 grams of body weight and euthanized 16 hours post injection. Tissue was harvested and fresh-frozen as described above.

CHAPTER III: GENERATION OF MINI DYSFERLIN gCAMP6 EXPRESSING CELL LINES FOR DOWNSTREAM MEMBRANE RESEALING ASSAY AND DEVELOPMENT OF MINI DYSFERLIN DELETION MUTANTS FOR GENE THERAPY

Introduction

As mentioned previously in the main introduction of this thesis, the discovery of a mini-dysferlin by Krahn et al 2010, which retains the membrane resealing function led to the possibility of mini dysferlin gene replacement therapy for Dysferlinopathy, due to limited AAV packaging capacity for full-length dysferlin cDNA. However, a recent report suggests a lack of correlation exists between rescue of membrane resealing function and histological improvement in dysferlin null mouse skeletal muscle following mini-dysferlin AAV treatment (32). The repair assay used in this study measured FM1-43 fluorescence uptake at the site of injury. The assumption that dye uptake directly correlates with membrane resealing may not be valid. It is possible that FM1-43 dye uptake at the site of injury does not directly measure resealing and therefore is not predictive of therapeutic outcome. One goal of this study is to develop tools for a downstream bioassay that directly measures membrane resealing by calcium influx to assess mini-dysferlin AAV treatment in dysferlin -/- Bla/J mice that were characterized.

The final goal of this study is to create mini dysferlin deletion mutations packaged into AAV and to validate expression *in vivo* using the Bla/J dysferlin null mouse model characterized.

Results

Development of gCaMP6s-expressing Dysferlin -/- Patient Myoblast Cell Lines

The gCaMP family of genetically encoded calcium indicator proteins are now widely used to measure calcium transients (34,35,36,37). The gCaMP protein is a fusion between circularly permutated GFP, calmodulin calcium binding domain, and M13 synthetic peptide(34,35,36,37).In the presence of calcium, a conformational change occurs in gCaMP, which causes the emission of GFP fluorescence. These unique properties of gCaMP were exploited for *in vitro* imaging of calcium transients in differentiated skeletal muscle cells after the cells were transduced with lentivirus carrying gCaMP6s, the latest, most sensitive, version of the gCaMP proteins. In Figure 4A, gCaMP6s fluorescence is observed 5 seconds post razor blade scratch injury to the cell. After 5 minutes post injury, the gCaMP6s signal returns to baseline in the part of the cell that did not detach from the plate post scratch injury. This simple proof-of-concept experiment confirms that gCaMP6s can be utilized to measure calcium transients in skeletal muscle. gCaMP6s was then introduced to dysferlin null patient myoblast 379 line through lentivirus infection (Figure 4B). Dysferlin deletion mutants were then introduced to the gCaMP6s-dysferlin null 379 cell line (Figures 4C & 4D). Five gCaMP6s-mini dysferlin expressing cell lines were created to test the membrane resealing capacity of each mini dysferlin deletion mutant using gCaMP6s as a reporter of calcium influx after sarcolemmal injury.

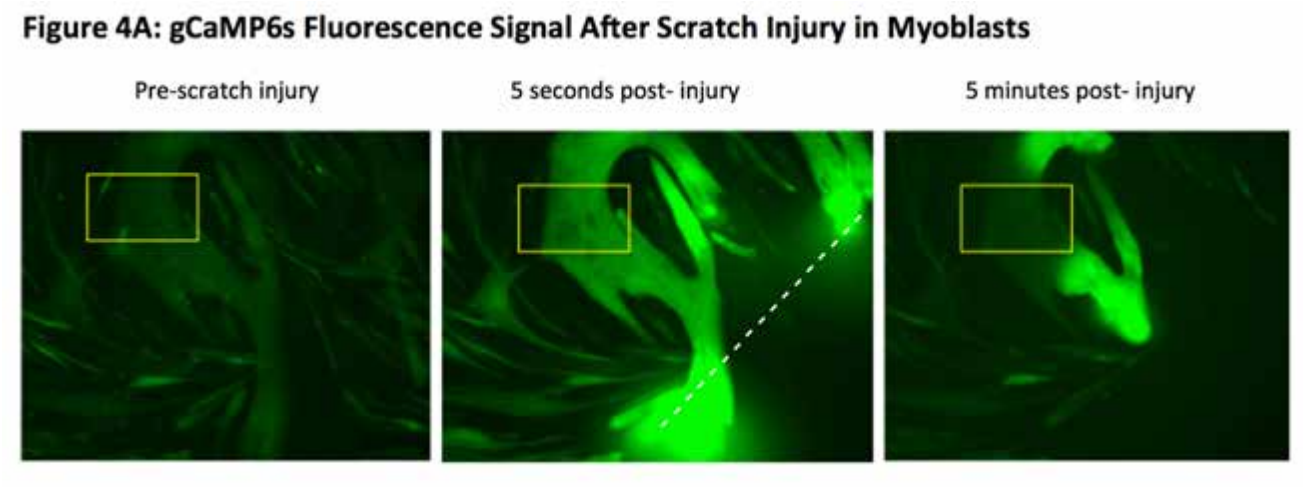

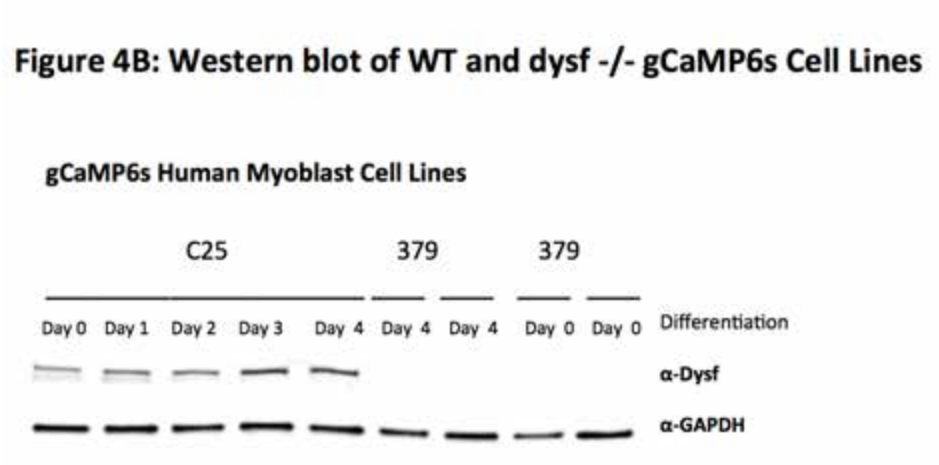

Figure 4A: gCaMP6s fluorescence transient in a WT C25 human myoblast differentiated cell line. The white broken line in the middle panel denotes the razor scratch injury trajectory. The yellow box denotes a region in the myofiber where it is intact from razor damage where the calcium transient after injury can be observed.

Figure 4B: A western blot confirming dysferlin expression in WT C25 myoblasts and confirming dysferlin loss in dysferlin null 379 myoblasts from differentiation day 0-4.

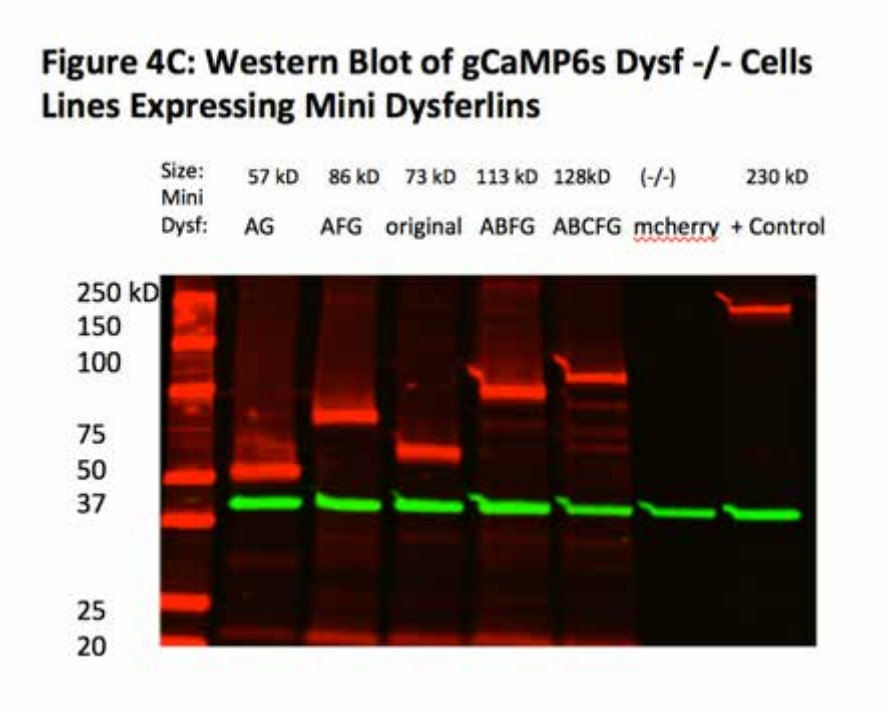

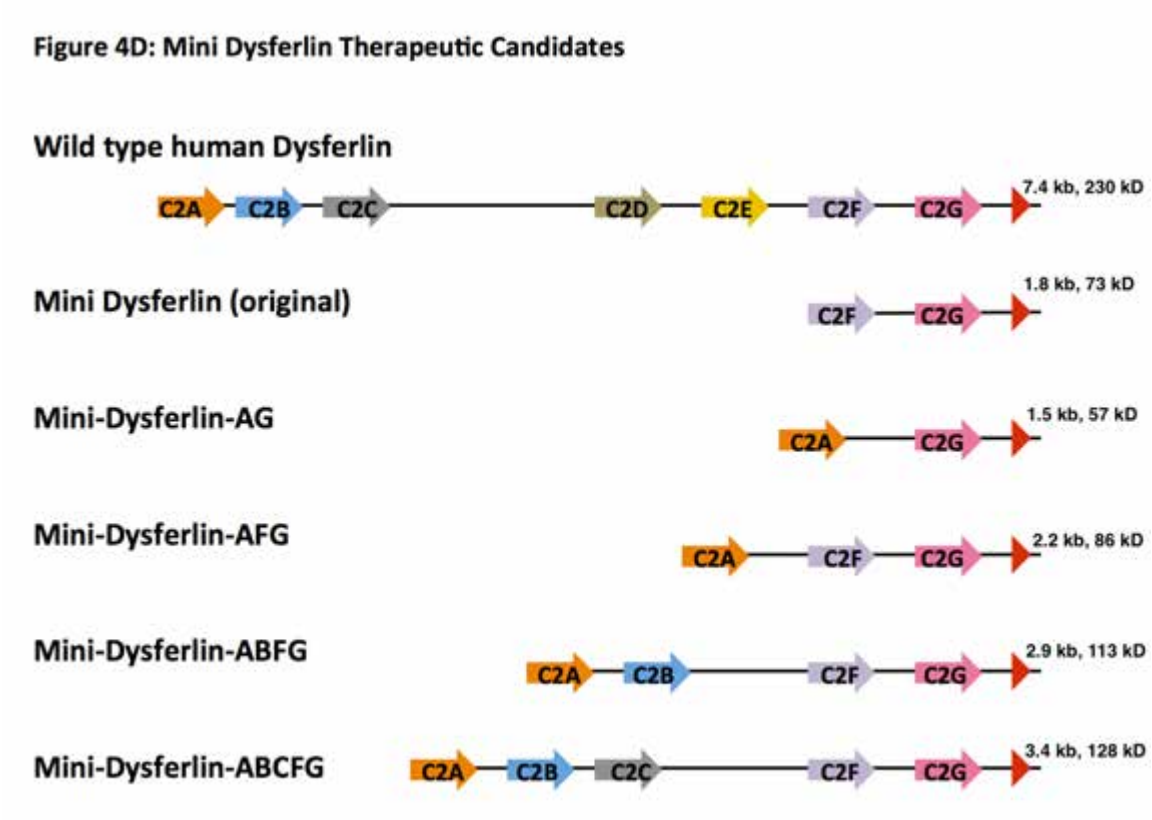

Figure 4C: Western blot confirming mini dysferlin deletion mutant expression in gCaMP6s dysferlin null cell line 379, after lentivirus transduction of each mini dysferlin.
Figure 2D: Map of dysferlin domains present in each mini dysferlin deletion mutant.

Mini Dysferlin Localization in gCaMP6s-dysferlin Null 379 Cell Line

After introducing each mini dysferlin to gCaMP6s-dysferlin null 379 cell line, five separate cell lines were created and mini dysferlin localization was assessed in each.

When cell lines were probed with dysferlin antibody NCL-Hamlet, which recognizes the C-terminus of WT dysferlin (present in all deletion mutants), a punctate staining pattern appeared for all deletion mutants (Figure 5A). The mini dysferlins do not seem to be present in the membrane, in contrast to WT dysferlin and dystrophin staining (Figure 5A). However, a different staining pattern emerges when some mini dysferlin cell lines were probed with NCL-Romeo, a dysferlin antibody that recognizes the N-terminus (Figure 5B). The staining pattern of the mini dysferlin cell lines probed with Romeo resemble WT dysferlin cell line staining and dystrophin staining shown in (Figure 5A). This difference suggests that dysferlin may be cleaved and only a part of the truncated protein localizes to the membrane.

AAV9-mediated Mini Dysferlin Delivery to Dysferlin -/- Bla/J Mice Skeletal Muscles

Mini dysferlin mutants were cloned into AAV vectors and packaged into AAV9 serotype. Bilateral intramuscular injections were carried out at $1.5x10^{11}$ vector genomes dosage in the quadriceps and gastrocnemius muscles of dysferlin null Bla/J mice (n=3 per mini dysferlin). Tissue was harvested 3 weeks post injection. Surprisingly, no transgene expression was observed by western blot (Figure 6) or immunostaining muscle sections(data not shown). The experiment was repeated with two more cohorts of mice including n=3 for each mini dysferlin and no transgene expression was observed.

Figure 5A: Mini Dysferlin Localization in Dysf -/- Myoblasts

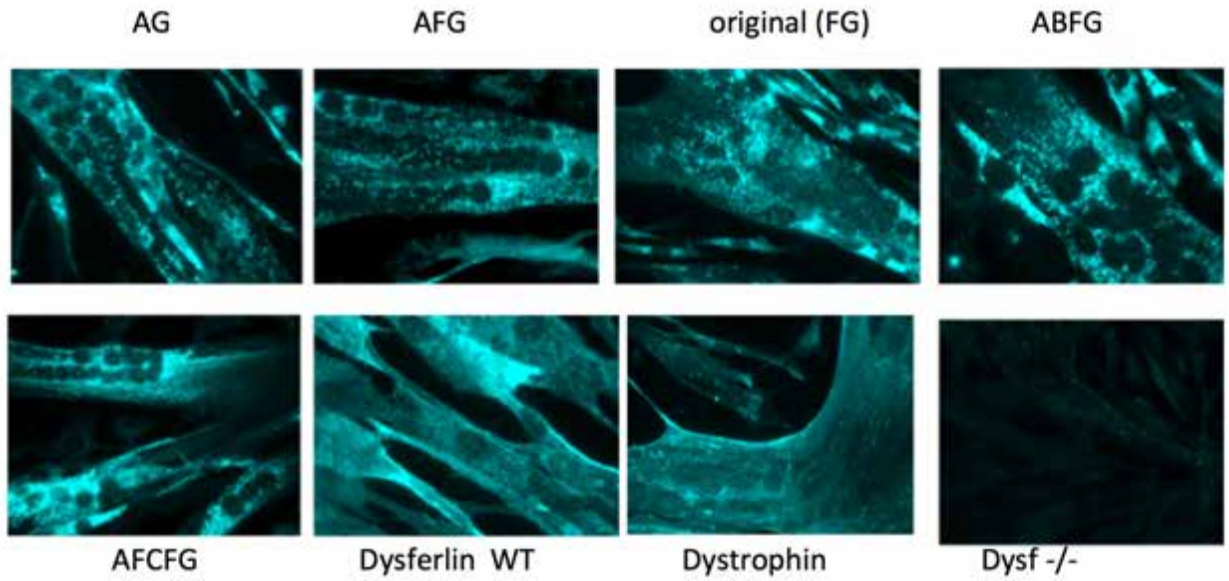

Figure 5B: Comparison of Mini Dysferlin Localization in Dysf -/- Myoblasts with different α-dysferlin antibodies

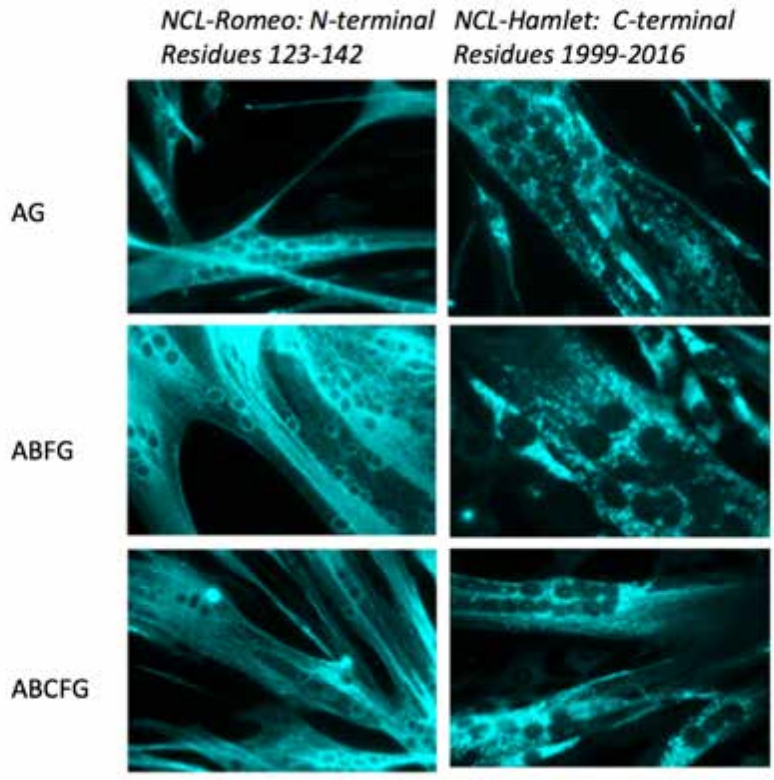

Figure 5A: Mini dysferlin punctate staining pattern in myotubes when probed with NCL-Hamlet.
Figure 5B: Comparison of mini dysferlin staining patterns when probed with C-terminus and N-terminus recognizing antibodies.

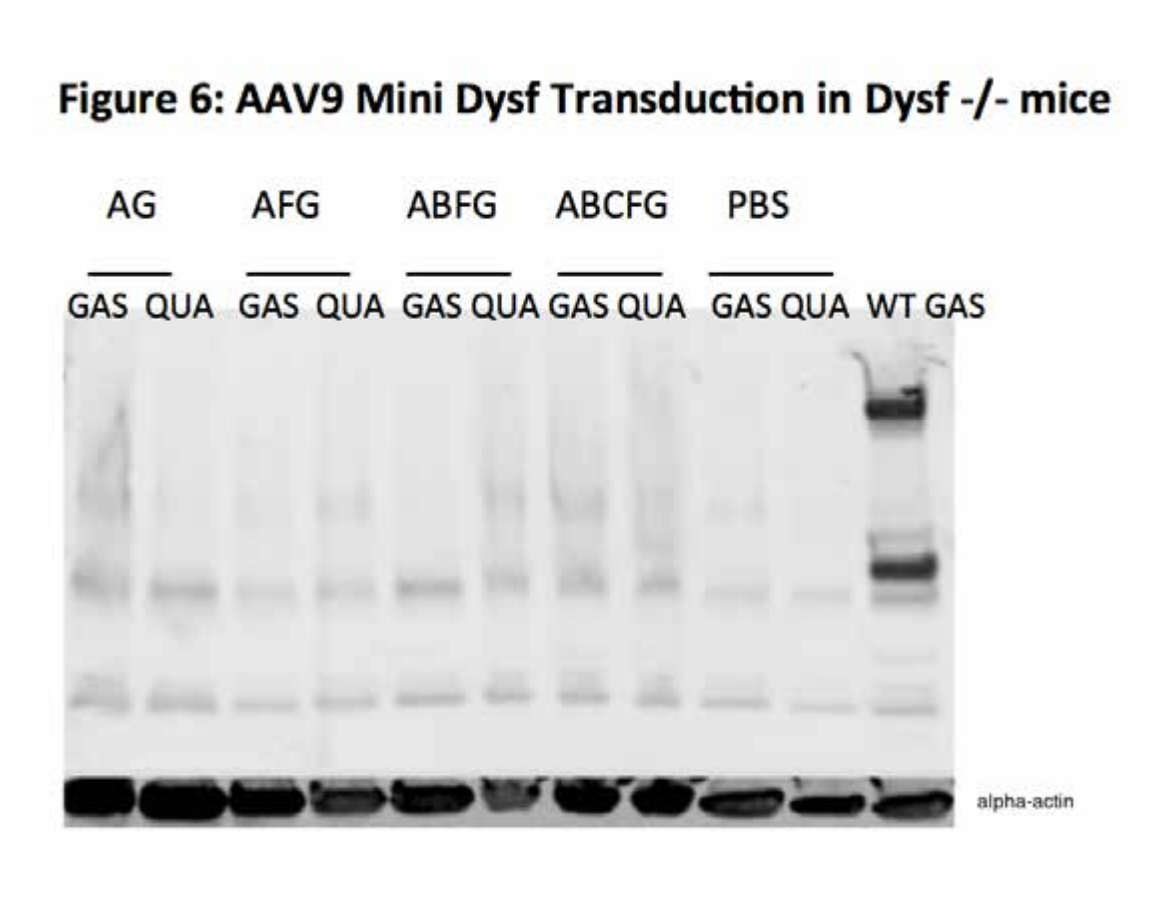

Figure 6: Western blot showing no mini dysferlin expression in mouse gastrocnemius and quadriceps muscles injected with AAV9 carrying mini dysferlin constructs.

Materials and Methods

Cloning

CMV- gCaMP6s sequence was amplified from pGP-CMV-GCaMP6s vector (Addgene #40753) with forward primer 5'-TTCGGGACCCATAGTAATCAATTACGGGGTCAT - 3' incorporating a PpuMI restriction site and reverse primer 5'-TGGGAATTCTCACTT CGCTGTC-3' containing an EcoRI restriction site. The 1.9 kb amplicon was amplified using Phusion High Fidelity DNA Polymerase (NEB #M0530S) and digested with PpuMI and EcoRI restriction endonucleases (NEB #R0506S, #R3101S) and column purified. pLKO.1hygro vector (Addgene ##24150) was also digested with PPuMI and EcoRI restriction ezymes and a 7 kb backbone was extracted from an agarose gel after electrophoresis. Amplified CMV-gCaMP6s fragment was ligated with pLKO.1 hygro vector at a 3:1 insert:vector ratio using T4 DNA ligase (NEB #M0202S). The plasmid was transformed into Stbl3 competent *E. coli* cells (Invitrogen #C737303). After propagation and purification from Stbl3 cells, pLKO.1hygro-CMV-gCaMP6s was sequenced.

Mini Dysferlins were cloned from full-length dysferlin cDNA into lentivirus vector CSCW2-IRES-mcherry using forward primer 5'-aaaaggtctcGCTAGCGCCACCATGCT GAGGGTC-3' with NheI restriction site and reverse primer 5'- aaaaggtctcCTCGAGTC AGCTGAAGGGCTTCACC-3' with XhoI restriction site (NEB# R0131S, R0146S). Amplified mini dysferlins and CSCW2-IRES-mcherry vector were digested with NheI and XhoI restriction enzymes and fragments were extracted from agarose gel based on size. Each mini dysferlin was ligated with the vector backbone at 3:1 ratio using T4 DNA ligase. Plasmids were transformed into Stbl3 cells, propagated, purified, and sequenced.

Mini dysferlin sequences were cloned out of lentivirus vectors and into a pAAV vector backbone with the NheI and XhoI restriction sites for AAV packaging. After ligation with T4 DNA ligase, plasmids were transformed into SURE2 competent cells (Agilent # 200152), propagated, and sequenced.

Lentivirus Production and Cell Line Generation

pLKO.1hygro-CMV-gCaMP6s and all CSCW2-CMV-Mini Dysferlin-IRES-mcherry constructs were packaged into lentivirus using the most recent protocol adapted from Molecular Cloning 4th edition volume 2. gCaMP6s expressing cells were created by lentivirus infection of pLKO.1hygro-CMV-gCaMP6s into dysferlin null patient cells (379) and WT control (C25) and both cell lines were subjected to hygromycin selection. After selection, 379-gcamp6s cells were infected with lentivirus packaged with dysferlin deletion mutants (CSCW2-CMV-minidysf-IRES-mcherry). Mcherry positive cells were FACS sorted. Myoblasts were cultured in 0.1% gelatin coated dishes with Promocell SGM proliferation medium, 20% FBS. Myoblasts were differentiated with Promocell Skeletal Muscle Differentiation medium. Immortalized human cell lines C25 and 379 were a gift from Vincent Mouly.

Western Blotting

Cell culture lysates were sonicated for 20 seconds and 20% amplitude in RIPA buffer. Tissue lysates were prepared by homogenization in T-PER buffer with a dounce homogenizer. BCA assays were used to determine protein concentration as per kit intstructions. Lysates were added to 2X Laemli buffer and boiled for 10 minutes at 70C. Boiled samples were then loaded to Bio-Rad precast gradient gels for electrophoresis. Proteins were transferred to nitrocellulose membranes using Invitrogen iBlot system and probed with anti-dysferlin antibody NCL-Hamlet.

Immunostaining

Mini dysferlin-expressing and control myoblasts were cultured in gelatin coated MatTek (# P35G-1.0-20-C) and differentiated until day 4. On Day 4, cells were rinsed with 1X PBS, incubated with acetone for 5 minutes , rinsed again with 1X PBS, and blocked for 45 minutes with 10% goat serum.Cells were then incubated with primary antibody (NCL-Hamlet or Romeo) for 1 hour, rinsed 3 times with 1X PBS, and incubated for 45 minutes with secondary anti-mouse or anti-rabbit antibody conjugated to Molecular Probes Alexa-Fluor 690. Plates were imaged using Nikon Ti Fluorescent microscope.

AAV9 Mini dysferlin delivery

Two milligrams of mini dysferlin cDNA in pAAV backbone were purified using Qiagen Endotoxin free Mega-Prep kit (#12381) and submitted to the UMass Medical School Gene Therapy Core Facility for packaging into AAV9.

CHAPTER IV: DISCUSSION

This thesis lays down the groundwork for a pre-clinical study in dysferlin null Bla/J mice to assess mini dysferlin therapeutic efficacy for dysferlin deficient muscular dystrophy gene therapy. This study has identified the muscle groups in the dysferlin null Bla/J mouse model with the most severe histological phenotype (triceps and quadriceps) and most severe loss of membrane integrity phenotype (gastrocnemius and quadriceps).

The severe histological phenotype observed in both quadriceps and triceps at 18 months could be due to the utilization of these muscles by the mice to support their body weight. The quadriceps seem to be the muscle group most widely utilized for both support of body weight and locomotion, thus it displays accelerated disease progression in comparison to the other groups characterized. These results suggest that the quadriceps is the ideal muscle group for phenotype evaluation after therapeutic intervention since it displays the most severe histological phenotype and loss of membrane integrity. Loss of membrane integrity appearing in the gastrocnemius without the same degree of histological severity as the quadriceps or triceps could be due to its primary function, which involves running and jumping that constantly stress the muscle fibers making them more permeable. The results from this study suggest that disease progression varies among muscle groups, and this may be explained by muscle function, physiology, and utilization by the mice.

This study characterized disease onset, progression, and endpoint in the Bla/J mouse. Taken together, this phenotype and disease progression characterization will be critical for establishing start points and endpoints of a pre-clinical study in these mice to assess a potential reversal of the dystrophic phenotype mediated by a mini dysferlin construct with therapeutic efficacy.

This study has also laid down the groundwork for elucidating dysferlin membrane resealing function and C2 domain function. gCaMP6s-mini dysferlin

expressing cell lines can be utilized for a more advanced membrane resealing assay using a laser-induced focal injury to the membrane to evaluate mini dysferlin resealing capacity measured directly by calcium influx. These future studies will shed light on the dysferlin membrane resealing function controversy in the field. Results from mini dysferlin localization studies with different staining patterns observed with two different anti dysferlin antibodies suggest that the protein may be cleaved and this cleavage might affect localization. A study in 2013 by Lek et al, showed compelling evidence that dysferlin is cleaved at the C-terminus after injury to the membrane. When the site of injury was probed with 3 different anti-dysferlin antibodies (one against the C-terminus and two against the N-terminus), only C-terminus dysferlin co-localized with the injury site. Furthermore, western blot analysis of injured myotubes showed the presence of a small 72 kD C-terminus dysferlin fragment that was absent in uninjured controls. Further co-localization studies can be performed with the mini dysferlin cell lines described in this thesis to uncover dysferlin protein biology and its role in membrane resealing.

It is imperative that mini dysferlin constructs in AAV vectors created are further improved by altering the promoter and AAV serotype to confirm robust transgene expression *in vivo* and assess therapeutic efficacy. In all, this thesis has uncovered the dystrophic disease progression in a mouse model mimicking the human disease in addition to constructing important elements for downstream pre-clinical and biological studies that will surely contribute to the Dysferlin field.

References

1.) Griggs, Robert C., and Anthony A. Amato. 2011. Muscular dystrophies. Edinburgh: Elsevier.
2.) Karpati, George. 2010. Disorders of voluntary muscle. Cambridge: Cambridge University Press.
3.) Liu J, M Aoki, I Illa, C Wu, M Fardeau, C Angelini, C Serrano, et al. 1998. "Dysferlin, a novel skeletal muscle gene, is mutated in Miyoshi myopathy and limb girdle muscular dystrophy". Nature Genetics. 20 (1): 31-6.
4.) Lennon NJ, A Kho, BJ Bacskai, SL Perlmutter, BT Hyman, and Brown RH Jr. 2003. "Dysferlin interacts with annexins A1 and A2 and mediates sarcolemmal wound-healing". The Journal of Biological Chemistry. 278 (50): 50466-73.
5.) Bansal D, K Miyake, SS Vogel, S Groh, CC Chen, R Williamson, PL McNeil, and KP Campbell. 2003. "Defective membrane repair in dysferlin-deficient muscular dystrophy". Nature. 423 (6936): 168-72.
6.) Glover L, and Brown RH Jr. 2007. "Dysferlin in membrane trafficking and patch repair". Traffic (Copenhagen, Denmark). 8 (7): 785-94.
7.) Achanzar WE, and S Ward. 1997. "A nematode gene required for sperm vesicle fusion". Journal of Cell Science. 110: 1073-81.
8.) Lek A, FJ Evesson, RB Sutton, KN North, and ST Cooper. 2012. "Ferlins: regulators of vesicle fusion for auditory neurotransmission, receptor trafficking and membrane repair". Traffic (Copenhagen, Denmark). 13 (2): 185-94.
9.) Roux I, S Safieddine, R Nouvian, M Grati, MC Simmler, A Bahloul, I Perfettini, et al. 2006. "Otoferlin, defective in a human deafness form, is essential for exocytosis at the auditory ribbon synapse". Cell. 127 (2): 277-89.
10.) Johnson CP, and ER Chapman. 2010. "Otoferlin is a calcium sensor that directly regulates SNARE-mediated membrane fusion". The Journal of Cell Biology. 191 (1): 187-97.
11.) Fernández-Chacón R, A Königstorfer, SH Gerber, J García, MF Matos, CF Stevens, N Brose, J Rizo, C Rosenmund, and TC Südhof. 2001. "Synaptotagmin I functions as a calcium regulator of release probability". Nature. 410 (6824): 41-9.
12.) Steinhardt, R., G Bi, and J. Alderton. 1994. "Cell membrane resealing by a vesicular mechanism similar to neurotransmitter release". Science. 263 (5145): 390-393.
13.) McNeil PL. 2002. "Repairing a torn cell surface: make way, lysosomes to the rescue". Journal of Cell Science. 115 (Pt): 873-9.
14.) McNeil PL, and M Terasaki. 2001. "Coping with the inevitable: how cells repair a torn surface membrane". Nature Cell Biology. 3 (5): 124-9.
15.) Miyake K, and PL McNeil. 1995. "Vesicle accumulation and exocytosis at sites of plasma membrane disruption". The Journal of Cell Biology. 131 (6): 1737-45.
16.) Reddy A, EV Caler, and NW Andrews. 2001. "Plasma membrane repair is mediated by Ca(2+)-regulated exocytosis of lysosomes". Cell. 106 (2): 157-69.
17.) Steinhardt RA. 2005. "The mechanisms of cell membrane repair: A tutorial guide to key experiments". Annals of the New York Academy of Sciences. 1066: 152-65.
18.) McNeil PL, and R Khakee. 1992. "Disruptions of muscle fiber plasma membranes. Role in exercise-induced damage". The American Journal of Pathology. 140 (5): 1097-109.
19.) Han WQ, M Xia, M Xu, KM Boini, JK Ritter, NJ Li, and PL Li. 2012. "Lysosome fusion to the cell membrane is mediated by the dysferlin C2A domain in coronary arterial endothelial cells". Journal of Cell Science. 125 (Pt): 1225-34.

20.) Hernández-Deviez DJ, S Martin, SH Laval, HP Lo, ST Cooper, KN North, K Bushby, and RG Parton. 2006. "Aberrant dysferlin trafficking in cells lacking caveolin or expressing dystrophy mutants of caveolin-3". Human Molecular Genetics. 15 (1): 129-42.
21.) Cai C, N Weisleder, JK Ko, S Komazaki, Y Sunada, M Nishi, H Takeshima, and J Ma. 2009. "Membrane repair defects in muscular dystrophy are linked to altered interaction between MG53, caveolin-3, and dysferlin". The Journal of Biological Chemistry. 284 (23): 15894-902.
22.) Waddell LB, FA Lemckert, XF Zheng, J Tran, FJ Evesson, JM Hawkes, A Lek, et al. 2011. "Dysferlin, annexin A1, and mitsugumin 53 are upregulated in muscular dystrophy and localize to longitudinal tubules of the T-system with stretch". Journal of Neuropathology and Experimental Neurology. 70 (4): 302-13.
23.) Krahn M., Wein N., Bartoli M., Courrier S., Nguyen K., et al. 2010. "A naturally occurring human minidysferlin protein repairs sarcolemmal lesions in a mouse model of dysferlinopathy". Science Translational Medicine. 2 (50).
24.) Lek A, FJ Evesson, FA Lemckert, GM Redpath, AK Lueders, L Turnbull, CB Whitchurch, KN North, and ST Cooper. 2013. "Calpains, cleaved mini-dysferlinC72, and L-type channels underpin calcium-dependent muscle membrane repair". The Journal of Neuroscience : the Official Journal of the Society for Neuroscience. 33 (12): 5085-94.
25.) Clark K.R., and Penaud-Budloo M. 2011. "Evaluation of the fate of rAAV genomes following in vivo administration". 807.
26.) Weitzman M.D., and Linden R.M. 2011. "Adeno-associated virus biology". Methods in Molecular Biology. 807: 1-23.
27.) Fields, Bernard N., David M. Knipe, Peter M. Howley, and Diane E. Griffin. 2002. Fields virology, fourth edition. Philadelphia, PA: Lippincott Williams & Wilkins.
28.) Gruntman AM, LT Bish, C Mueller, HL Sweeney, TR Flotte, and G Gao. 2013. "Gene transfer in skeletal and cardiac muscle using recombinant adeno-associated virus". Current Protocols in Microbiology. Chapter.
29.) Lostal W, M Bartoli, N Bourg, C Roudaut, A Bentaïb, K Miyake, N Guerchet, F Fougerousse, P McNeil, and I Richard. 2010. "Efficient recovery of dysferlin deficiency by dual adeno-associated vector-mediated gene transfer". Human Molecular Genetics. 19 (10): 1897-907.
30.) Grose WE, KR Clark, D Griffin, V Malik, KM Shontz, CL Montgomery, S Lewis, et al. 2012. "Homologous recombination mediates functional recovery of dysferlin deficiency following AAV5 gene transfer". PloS One. 7 (6).
31.) Lai Y, Y Yue, and D Duan. 2010. "Evidence for the failure of adeno-associated virus serotype 5 to package a viral genome > or = 8.2 kb". Molecular Therapy : the Journal of the American Society of Gene Therapy. 18 (1): 75-9.
32.) Lostal W, M Bartoli, C Roudaut, N Bourg, M Krahn, M Pryadkina, P Borel, et al. 2012. "Lack of correlation between outcomes of membrane repair assay and correction of dystrophic changes in experimental therapeutic strategy in dysferlinopathy". PloS One. 7 (5).
33.) Mengfatt Ho,Cristina M. Post, Leah R. Donahue, Hart G.W. Lidov, Roderick T. Bronson,Holly Goolsby,Simon C. Watkins, Gregory A. Cox, and Robert H. Brown

Jr.2004.” Disruption of muscle membrane and phenotype divergence in two novel mouse models of dysferlin deficiency”.Human Molecular Genetics. 14 (18):1999-2010.

34.) Akerboom J, JD Rivera, MM Guilbe, EC Malavé, HH Hernandez, L Tian, SA Hires, JS Marvin, LL Looger, and ER Schreiter. 2009. "Crystal structures of the GCaMP calcium sensor reveal the mechanism of fluorescence signal change and aid rational design". The Journal of Biological Chemistry. 284 (10): 6455-64.
35.) McCombs JE, and AE Palmer. 2008. "Measuring calcium dynamics in living cells with genetically encodable calcium indicators". Methods (San Diego, Calif.). 46 (3): 152-9.
36.) Mank M, and O Griesbeck. 2008. "Genetically encoded calcium indicators". Chemical Reviews. 108 (5): 1550-64.
37.)Kotlikoff MI. 2007. "Genetically encoded Ca2+ indicators: using genetics and molecular design to understand complex physiology". The Journal of Physiology. 578 (Pt): 55-67.

38.)Deyle DR, and Russell DW. 2009. “Adeno-associated virus vector integration”. Current Opinion Molecular Therapy . 11(4): 442-447.